Scaling laws for fully developed turbulent flow in pipes*

GI Barenblatt, AJ Chorin

Department of Mathematics and Lawrence Berkeley Laboratory, University of California, Berkeley CA 94720

VM Prostokishin

PP Shirshov Institute of Oceanology, Russian Academy of Sciences, Moscow 117218 Russia

Mathematical and experimental evidence is presented to the effect that the velocity profile in the intermediate region of turbulent shear flow in a pipe obeys a Reynolds-number dependent scaling (power) law rather than the widely believed von Kármán-Prandtl universal logarithmic law. In particular, it is shown that similarity theory and the Izakson-Millikan-von Mises overlap argument support the scaling law at least as much as they support the logarithmic law, while the experimental evidence overwhelmingly supports the scaling law. This review article includes 39 references

1 INTRODUCTION

Turbulent flow in pipes is among the flows most important to humans, in engineering practice and elsewhere. It has been the object of much attention and its properties are widely taught. It is therefore particularly surprising that a widely used description of that flow by means of the von Kármán-Prandtl universal logarithmic law of the wall should be inappropriate. We shall show this to be the case, and we shall show that another description, by a certain Reynolds-number dependent scaling (power) law, constitutes a substantial improvement. It is ironical that power laws had been used by engineers before theoreticians persuaded them that they should be abandoned.

Consider a long cylindrical pipe with a circular cross-section, and the time-averaged flow in its working section, *ie*, far from its inlet and outlet. The emphasis will be on the time-averaged flow rather than on the instantaneous flow, because instantaneous flow varies sharply in both space and time, its analysis requires advanced tools that are not yet available, and it is not of prime concern in practical problems. By contrast, the averaged values are useful, reproducible, and form relatively simple patterns.

Since the days of Reynolds, data about turbulent flow are presented in a dimensionless form, making possible a unified description of flows of different fluids (for example, air and water), in pipes of various diameters, etc. This dimensionless description should be independent of the choice of the magnitude of the basic units of measurement. In particular, it is customary to represent the average longitudinal velocity u as

$$\phi = u / u_* \tag{1.1}$$

where u_* is the *dynamic* or *friction* velocity that defines a velocity scale:

$$u_* = \sqrt{\tau/\rho}, \tag{1.2}$$

where ρ is the density of the fluid and τ is the shear stress at the pipe's wall determined as

$$\tau = \frac{\Delta p}{L}\frac{d}{4}. \tag{1.3}$$

Here Δp is the pressure drop over the working section of the pipe, L is the length of the working section, and d is the pipe's diameter. The dimensionless distance from the pipe wall is represented as

$$\eta = \frac{u_* y}{\nu} \tag{1.4}$$

where y is the actual, dimensional distance from the wall and ν is the kinematic viscosity. Note that the natural length scale ν/u_* used in (1.4) is typically very small – of the order of tens of microns or even less in some of the experiments described below.

The basic dimensionless parameter of the problem is the Reynolds number

$$Re = \frac{\overline{u} d}{\nu} \tag{1.5}$$

where $\overline{u}$ is the mean velocity averaged over the cross-section, *ie*, the time-averaged fluid flux (discharge rate) divided by the area of the cross-section. The Reynolds number (1.5) can be viewed as the ratio of d and a second natural length scale $\nu/\overline{u}$, which is much smaller yet than ν/u_*.

When the Reynolds number Re is large, one observes that the cross-section is divided into three parts (Fig 1): a thin ring (1) near the wall, where the velocity gradient is so large that the shear stress due to molecular viscosity, *ie*, the rate of momentum transfer by the thermal motion of the fluid's molecules, is comparable to the turbulent shear stress, *ie*, to

Transmitted by Associate Editor SA Berger

* Supported in part by the Applied Mathematical Sciences subprogram of the Office of Energy Research, USDoE, under contract DE-AC03-76-SF00098, and in part by the National Science Foundation under grants DMS94-14631 and DMS89-19074.

ASME Reprint No AMR217 $18

the rate of momentum transfer due to the turbulent vortices. This is the *viscous sublayer*. In a cylinder (2) surrounding the pipe's axis, the velocity gradient is small, and the average velocity is close to its maximum. Our analysis will focus on the *intermediate region* (3) which occupies the major part of the cross-section.

During the more than 60 years of active research into turbulent pipe flow, two contrasting laws for the velocity distribution in the intermediate region have coexisted in the literature (see, *eg* Schlichting [35]): the first is the power or *scaling* law,

$$\phi = C\eta^{\alpha} \tag{1.6}$$

where the C and α are constants (*ie* parameters independent of η) believed to depend weakly on Re. Laws such as (1.6) were in particular proposed by engineers in the early years of turbulence research. The second law found in the literature is the *universal*, Reynolds number independent logarithmic law,

$$\phi = \frac{1}{\kappa}\ln\eta + B \tag{1.7}$$

where κ (von Kármán's constant) and B are assumed to be *universal, ie Re*-independent, constants.

In more recent decades, the logarithmic law (1.7) has been emphasized over the power law (1.6), sometimes even to the exclusion of the latter. The reasons have been mainly theoretical: it was not recognized that the power law has an equally valid theoretical derivation and satisfies the appropriate self-consistency (*overlap*) condition. This theoretical bias has been allowed to obscure the fact that the experimental data unequivocally militate in favor of the power law (1.6).

A commonly-accepted derivation of the universal logarithmic law (1.7), due originally to von Kármán [25] and Prandtl [33], and, its final form, to Landau and Lifshitz [28], proceeds as follows: Assume that the velocity gradient $\partial_y u, \left(\partial_y \equiv \frac{\partial}{\partial y}\right)$ in the intermediate region (3) of Fig 1 depends on the following variables: the coordinate y, the shear stress at the wall τ, the pipe diameter d, and the properties of the fluid, specifically, its kinematic viscosity ν and density ρ. We choose to consider the velocity gradient $\partial_y u$ rather than u itself because the values of u depend on the flow in the viscous sublayer where the basic assumptions we shall use are not valid. Thus

$$\partial_y u = f(y, \tau, d, \nu, \rho) \tag{1.8}$$

Dimensional analysis (see the next section) gives

$$\partial_y u = \frac{u_*}{y}\Phi(\eta, Re), \quad Re = \frac{\overline{u}d}{\nu}, \quad \eta = \frac{u_* y}{\nu}, \tag{1.9}$$

where Φ is a dimensionless function of its arguments, which remains undetermined at this stage. The same kind of dimensional analysis gives for the "friction" velocity

$$\frac{u_* d}{\nu} = \frac{\overline{u}d}{\nu}\cdot F(Re), \tag{1.10}$$

where F is a dimensionless function of its argument and the Reynolds number Re is given by equation (1.5). Thus equation (1.8) can be rewritten in the form

$$\partial_\eta \phi = \frac{1}{\eta}\Phi(\eta, Re), \quad \phi = \frac{u}{u_*}. \tag{1.11}$$

Outside the viscous sublayer η is large, of the order of several tens and more; in the kind of turbulent flow we wish to consider the Reynolds number Re is also large, of the order of 10^4 at least. It may therefore have been natural to assume that for such large values of η and Re the function Φ no longer varies with its arguments and can be replaced by its limiting value $\kappa^{-1} = \Phi(\infty, \infty)$. Substitution into (1.11) yields

$$\partial_\eta \phi = \frac{1}{\kappa\eta}, \tag{1.12}$$

and an integration then yields the logarithmic law (1.7). However, as we shall see in detail below, there is no over-

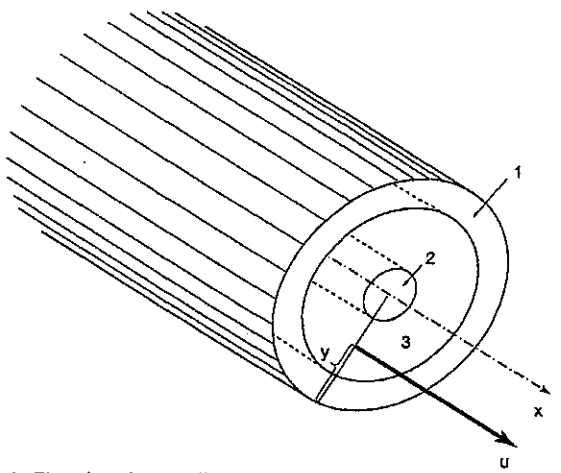

Fig 1. Flow in a long cylindrical pipe: structure at large Reynolds number: 1) Viscous sublayer, 2) Near-axis region, and 3) Intermediate region

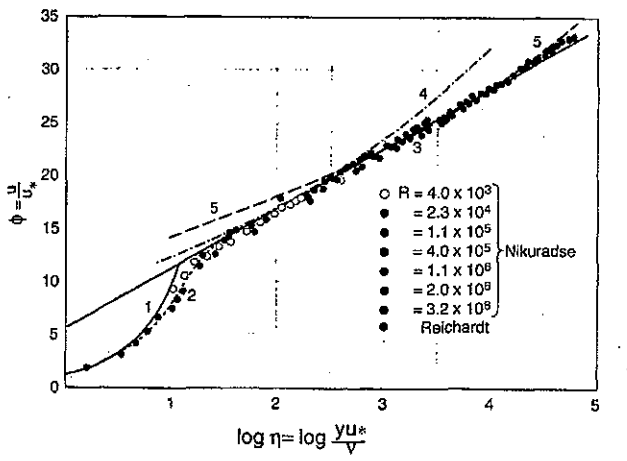

Fig 2. Comparison of the universal logarithmic law with experiment: (after Schlichting [36]): 1) $\phi = \eta$ (sublayer), 2) Transition from the viscous sublayer to the fully turbulent core, 3) Universal logarithmic law: ($\phi = 2.5\ln\eta + 5.5$), 4) $\phi = 8.74\eta^{1/7}$ (Blasius), 5) $\phi = 11.5\eta^{1/10}$

whelming reason to assume that the function Φ has a constant, non-zero limit as its arguments tend to infinity. When that limit does not exist other conclusions must be reached.

It is generally thought that the universal logarithmic law (1.7) is in satisfactory agreement with the experimental data both in pipes and in boundary layers. The graphs in Fig 2 (drawn after Schlichting [35]), and in Fig 3 (drawn after Monin and Yaglom [29]) have been adduced as evidence. However, the scaling law (1.6) has also found experimental support, provided the dependence of the quantities α and C on the Reynolds number was properly taken into account. Indeed, Schlichting, following Nikuradze, showed (Fig 4) that the experimental data agree with the scaling law over practically the whole cross-section of a pipe.

We now set out to determine which of these laws, if any, best describes turbulent flow of fluids such as air or water. This question is of great practical as well as theoretical significance. We proceed as follows. First, we present a short survey of dimensional analysis and of modern, advanced similarity methods; we use these techniques to present the derivation of the universal logarithmic law and of the scaling law as consequences of specific similarity assumptions within the framework of these methods. In the absence of further information, these derivations are equally convincing. We present a first processing of experimental data that shows that the scaling law, with a certain specific choice of constants, fits the data best. We then use vanishing-viscosity asymptotics to extrapolate our results to higher Reynolds numbers, to refine the comparison with experiment, and to show that the power law satisfies a version of the well-known *overlap* condition that is compatible with the data. Finally, we consider some recent experimental data, show that at low and moderate *Re* they confirm the scaling law with the right constants, but that at large *Re*, while these data still support a scaling law, our analytical tools reveal a major flaw in the experiment from which they originate.

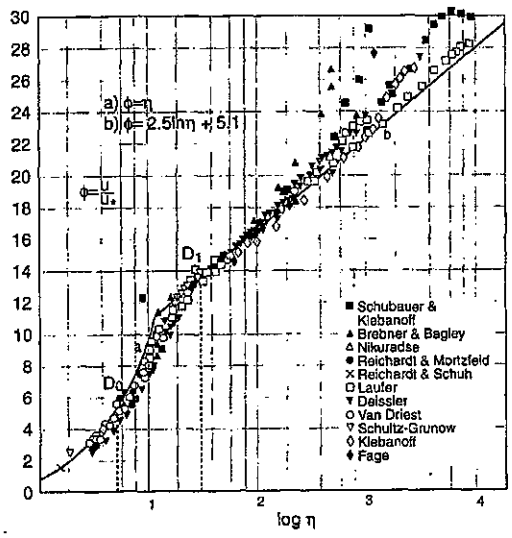

Fig 3. Comparison of the universal logarithmic law with experiment (after Monin and Yaglom [29])

Our conclusion is that the appropriate description of the intermediate region in turbulent pipe flow is given by the scaling law. This conclusion has far-reaching practical as well as theoretical consequences.

Some historical comments: The *overlap* argument of Izakson, Millikan and von Mises (IMM) (see [18], [29] and Section 5 below) is generally thought to have won the day for the logarithmic law so that even when data supporting the power law appeared, they were disregarded (this point is discussed in [37]); we shall show, following [4], [5], [6], that the IMM argument supports the power law at least as much as it supports the logarithmic law. Some recent books either omit the power law completely [28] or describe it as belonging to history ([29], p 309); this despite the steady stream of data that favor the power law (see *eg* [11], [21], [26], [36]) – a (temporary) victory of prejudice over fact. The specific form of the power law we shall end up with was first presented in [2], [3], [9]. A further processing of the data was performed in [7]. An illuminating survey of dimensionless variables in fluid mechanics and of their history can be found in [34].

2 SCALING LAWS AND ADVANCED SIMILARITY METHODS

Fluid dynamicists are familiar with the concept of dynamic Reynolds number similarity: If one has found a flow in a given geometry, with a length scale L, viscosity ν and velocity scale U, one can find a flow in a similar geometry, with a different length scale and a different viscosity, by scaling the velocity so that the Reynolds number $Re = UL/\nu$ is the same; in other words, if the length scale and the viscosity change, one can obtain a solution of the new problem by multiplying (*scaling*) the velocity field by the appropriate constant that keeps *Re* fixed. We wish to generalize this simple analysis of the effects of changes in scales.

Consider a physically meaningful relation between physical variables:

$$y = f(x_1, x_2, \ldots, x_k, c) \tag{2.1}$$

where the arguments x_1, x_2,... have independent dimensions while the dimensions of y and c are monomials in the powers of the dimensions of the x_i:

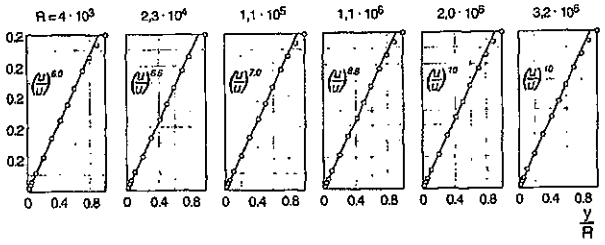

Fig 4. Data of Nikuradze [31] represented in a form showing that a proper choice of power allows one to describe the velocity distribution by a power law nearly across the entire cross-section (after Schlichting [35])

$$[y]=[x_1]^p\dots[x_k]^r,$$
$$[c]=[x_1]^q\dots[x_k]^s. \tag{2.2}$$

Here $[x]$ denotes the dimensions of the variable x and for simplicity we restrict ourselves to the case of a single independent variable c with dependent dimensions.

A physical relationship similar to (2.1) must be held for all observers even if they use a different system of physically equivalent units having different magnitudes. The change from one observer to another is expressed by the transformation of the values of y, $x_1,\dots,x_k$, c, of the form determined by the dimensions (2.2):

$$x_1'=A_1x_1,\ \dots,\ x_k'=A_kx_k,$$
$$y'=A_1^p\dots A_k^r y,\ \ c'=A_1^q\dots A_k^s c. \tag{2.3}$$

The quantities which remain invariant after the transition from one observer to the next are obviously

$$\Pi=\frac{y}{x_1^p\dots x_k^r},\ \ \Pi_1=\frac{c}{x_1^q\dots x_k^s};$$

thus the invariant form of equation (2.1) is

$$\Pi=\Phi(\Pi_1), \tag{2.4}$$

where Φ is a dimensionless function; a comparison of equations (2.1) and (2.4) shows that the function $f(x_1,\dots x_k,c)$ has the important generalized homogeneity property

$$f(x_1,\dots,x_k,c)=x_1^p\dots x_k^r\Phi\left(\frac{c}{x_1^q\dots x_k^s}\right) \tag{2.5}$$

These considerations belong to standard dimensional analysis.

Consider now what happens when the variable Π_1 is small, $\Pi_1 \ll 1$. In such cases one is accustomed to tell undergraduates that the function Φ can be replaced by the constant $C=\Phi(0)$ and the problem is greatly simplified. If this is indeed true, then for small enough Π_1 one can replace equation (2.1) by the simpler relation

$$y=Cx_1^p\dots x_k^r, \tag{2.6}$$

Here C is a single constant to be determined, and the parameter c completely disappears from the equation for small Π_1. The powers $p,\dots,r$ can be found by simple dimensional analysis. When this situation holds, one says that one has *complete similarity in the parameter* Π_1. The strong implicit assumption here is that as $\Pi_1 \to 0$, Φ tends to a constant non-zero limit C. This is exactly what was assumed in the derivation of the logarithmic law in the introduction. However, it is obvious that in general complete similarity does not hold; in general, there is no reason to believe that Φ has a finite non-zero limit when $\Pi_1 \to 0$, and the parameter Π_1, far from disappearing, may well become essential, even when, or particularly when, it is small.

Here there is an important special case. Assume that Φ has no non-zero finite limit when Π_1 tends to zero, but that in the neighborhood of $\Pi_1 = 0$ one has for Φ a representation as a power of the form

$$\Phi(\Pi_1)=C\Pi_1^\alpha+\dots, \tag{2.7}$$

for some C and α, where the dots represent smaller terms. Substituting (2.7) into (2.4) for Π_1 small we find

$$\Pi=C\Pi_1^\alpha, \tag{2.8}$$

or, returning to dimensional variables,

$$y=Cx_1^{p-\alpha q}\dots x_k^{r-\alpha s}c^\alpha, \tag{2.9}$$

ie, the power relation is of the same general form as in (2.6), but with two essential differences: The powers of the variables x_i, $i = 1,\dots,k$ cannot be obtained by dimensional analysis and must be derived by an additional, separate analysis, and the argument c has not disappeared from the resulting relation. We refer to such cases as cases of *incomplete similarity in the parameter* Π_1: A scaling law is obtained, but the parameter c does not disappear and enters that law, albeit only in a certain well-defined power combination with the parameters $x_1,\dots,x_k$. Although the determination of the parameter α requires an effort beyond dimensional analysis, the relation (2.9) has a *scaling* (power) form. Such scaling relations have a long history in engineering, where a widely-shared opinion held, until recently, that since they cannot be obtained from dimensional considerations, they were nothing more than empirical correlations. In fact they are merely a more complicated case of similarity.

The occurrence of incomplete similarity can remain hidden if one fails to perform a sufficiently thorough examination of a problem. For more information about similarity methods see [1].

3 SIMILARITY AND THE DERIVATION OF THE SCALING LAW AND OF THE LOGARITHMIC LAW

We now return to the derivation of the universal logarithmic law given in the introduction. It was already mentioned there that the relation (1.12) is derived from the basic relation (1.11) by assuming that the function $\Phi(\eta, Re)$ has, as $\eta \to \infty$ and $Re \to \infty$, a finite limit different from zero. Moreover, the passage from (1.11) to (1.12), from which the universal logarithmic law is obtained by integration, is based also on the assumption that both the Reynolds number Re and the values of η in the intermediate region are large enough for the function Φ to be replaced by its limit.

Our knowledge of the Navier-Stokes equations and of their solutions is not sufficient to decide whether such a limit exists. Assume to the contrary that this limit does not exist, but that at large η the function Φ can be represented as a power in the form:

$$\Phi(\eta,Re)=A\eta^\alpha+\text{smaller quantities}, \tag{3.1}$$

where the quantities A and $\alpha \neq 0$ are allowed to depend on the Reynolds number. In the language of the preceding section, we are assuming incomplete similarity in the parameter η and no similarity nor any other invariance in the parameter Re.

It is important to note that it is not the limit of $\Phi(\eta,Re)$ as $\eta \to \infty$ that is of interest, but the behavior of the basic equation (1.11) for large but finite values of η, when the points that correspond to these values are outside the viscous sublayer but not yet in the vicinity of the axis of the pipe. It is therefore possible to neglect the smaller quantities in (3.1) and write

$$\Phi = A\eta^{\alpha}, \tag{3.2}$$

so that

$$\partial_{\eta}\phi = A\eta^{\alpha-1}. \tag{3.3}$$

By integration, equation (3.3) yields

$$\phi = \frac{A}{\alpha}\eta^{\alpha} + \text{constant}. \tag{3.4}$$

The scaling law (1.6) is obtained if A/α is denoted by C and the additive constant is set equal to zero. This last condition is an important independent statement; it is not a consequence of the no-slip condition at the wall because equation (3.4) is not valid in the viscous sublayer near the wall. The ultimate justification for the dropping of the additive constant is a comparison with experiment.

An important conclusion has been reached: *The power law (1.6) and the logarithmic law (1.7) can be derived with equal rigor but from different assumptions.* The universal logarithmic law is obtained from the assumption of complete similarity in both parameters η and *Re*; physically, this assumption means that neither the molecular viscosity ν nor the pipe diameter d influences the flow in the intermediate region. The scaling law (1.6) is obtained from an assumption of incomplete similarity in η and no similarity in *Re*; this assumption means that the effects of both ν and d are perceptible in the intermediate region.

Note immediately a significant difference between the cases of complete and incomplete similarity. In the first case the experimental data should cluster, in the $(\ln\eta, \phi)$ plane ($\phi = u/u_*$, $\eta = u_*y/\nu$), on the universal straight line of the logarithmic law. In the second case the experimental points occupy an area in the $(\ln\eta, \phi)$ plane.

Both similarity assumptions are very specific. The possibility that Φ has no non-zero limit yet cannot be represented asymptotically as a power of η has not been excluded. Both assumptions must be subjected to careful scrutiny. In the absence of reliable, high-*Re* numerical solutions of the Navier-Stokes equation and of an appropriate rigorous theory, this scrutiny must be based on careful comparison with experimental data.

4 FURTHER SPECIFICATION OF THE SCALING LAW AND BASIC EXPERIMENTAL VERIFICATION

Under the assumption of incomplete similarity in η and lack of similarity in *Re*, we have arrived at the relation

$$\Phi(\eta,Re) = A(Re)\eta^{\alpha(Re)} \tag{4.1}$$

in conjunction with the general relations

$$\partial_y u = \frac{u_*}{y}\Phi(\eta,Re), \quad or \quad \partial_{\eta}\phi = \frac{1}{\eta}\Phi(\eta,Re). \tag{4.2}$$

The case of complete similarity in η and Re was considered in the introduction. Before proceeding to a comparison with experiment, we have to specify further the conditions under which we expect (4.1) to hold, and narrow down the possible choices for $A(Re)$ and $\alpha(Re)$.

We expect equations (4.1) and (4.2) to hold in fully developed turbulence. These equations depend on *Re*, and it is thus not consistent to view fully developed turbulence as a single, well-defined state with properties independent of *Re*. We may expect a single, well-defined, fully turbulent regime in the limit of infinite Reynolds number, but experience shows that what anyone would consider to be fully developed turbulence still exhibits a perceptible dependence on *Re*. We thus define fully developed turbulence as turbulence whose mean properties (for example, the parameters in (4.1)) vary with Reynolds number like $K_0 + K_1\varepsilon$, where K_0, K_1 are constants and ε is a small parameter that depends on *Re*, small enough so that its higher powers are negligible, yet not so small that its effects are imperceptible in situations of practical interest; the latter condition rules out choices such as $\varepsilon = (Re)^{-1}$. Under these conditions we expect $A(Re)$ and $\alpha(Re)$ in (4.1) to have the form

$$A(Re) = A_0 + A_1\varepsilon, \qquad \alpha(Re) = \alpha_0 + \alpha_1\varepsilon. \tag{4.3}$$

In formulating our definition of fully developed turbulence we have implicitly used *vanishing-viscosity asymptotics, ie*, we have used the fact that as the viscosity ν tends to zero those properties that we are examining have a well-defined limit. This limit exists in particular for moments of the velocity field, as long as they are not of too high an order. An analysis of this property, based on statistical mechanics arguments, has been given in [13], [14], [15], [16]. It is implicit in the work of Onsager [17], [32]. We shall draw a number of conclusions from the existence of the vanishing-viscosity limit; here the existence of the limit requires that $\varepsilon(Re) \to 0$ as $Re \to \infty$. Indeed, we formulate the existence of the vanishing-viscosity limit as a basic hypothesis:

Hypothesis: There exists a well-defined limit of the velocity gradient as the viscosity ν tends to zero.

To find the precise implications of this hypothesis, rewrite equation (4.1) in the form

$$\Phi = (A_0 + A_1\varepsilon)\exp(\alpha_0 \ln\eta + \alpha_1\varepsilon\ln\eta) \tag{4.4}$$

We see that as $\nu \to 0$, $Re \to \infty$, and a well defined limit in the argument of the exponential exists if and only if $\alpha_0 = 0$, and either $\varepsilon = \frac{1}{\ln Re}$ (the constant factor in ε can be taken equal to one because one can always rescale the constants α_1 and A_1), or $\frac{\varepsilon}{\ln Re} \to 0$ as $Re \to \infty$. Comparison with experimental data shows that the threshold choice $\varepsilon = \frac{1}{\ln Re}$ is the one to use; this is the choice that allows the largest effect of the Reynolds number on the mean properties of the turbulence without violating our basic principle.

Table 1. α as a function of Re (following Schlichting [35])

Re	α^{-1}
4×10^3	6.0
2.3×10^4	6.6
1.1×10^5	7.0
1.1×10^6	8.8
2.0×10^6	10
3.2×10^6	10

A further argument in favor of the specific choice $\varepsilon(Re) = \frac{1}{\ln Re}$ for the small parameter results is the *asymptotic covariance* of the resulting law [8], [22]. Equations (4.1)-(4.3) should be invariant under a change in the definition of Reynolds number, which contains an arbitrary choice of length scale and velocity scale. A change in these choices multiplies Re by a constant Z, and we expect formulas (4.3) to remain valid, with the same A_0, A_1, α_0, α_1 when Re is replaced by $Z \cdot Re$. (or else these constants too are functions of the choice of scales, and must be subjected to a scaling analysis that will bring us back to the form (4.1)). The obvious relation $\ln(ZRe) = \ln Re + \ln Z \sim \ln Re$ for large Re ensures that this is so. Thus

$$\Phi = \left(A_0 + \frac{A_1}{\ln Re}\right)\eta^{\frac{\alpha_1}{\ln Re}} \tag{4.5}$$

in the range of Re we shall be considering. Substitution of (4.5) into (4.1) and integration yields

$$\phi = \frac{u}{u_*} = \left(C_0 \ln Re + C_1\right)\eta^{\frac{\alpha_1}{\ln Re}} \tag{4.6}$$

where the additional condition $\phi(0) = 0$ has been used.

According to the logic of the derivation given above, the coefficients C_0, C_1, α_1 are universal constants, and should be the same in all past and all future experiments of sufficiently high quality performed in pipe flows at large Reynolds numbers. A decision was taken to compare the predicted scaling law for smooth walls (4.5) with what seemed to be the best available data, produced by Nikuradze [31] under the guidance of L Prandtl at his institute in Göttingen. It is particularly important that these data are available in tabular form and not only as graphs. The comparison was performed in several steps.

Step 1. Following Nikuradze, Schlichting [35] presented a best fit for $\alpha = \alpha(Re)$ in tabular form (Table I and Fig 4). A simple calculation shows that this table is in good agreement with the hypothesis $\alpha_0 = 0$, $\alpha_1 = 3/2$. We have already seen that the result $\alpha_0 = 0$ is in fact a consequence of a general principle, and the experimental verification of this conclusion is a check on the data.

Step 2. The preliminary result $\alpha(Re) = 3/2 \ln Re$ was subjected to an exhaustive verification. Indeed, if the scaling law (1.6) is valid, then the relation

$$\phi^{1/\alpha} = C^{1/\alpha}\eta \tag{4.7}$$

should hold, where C is a function of Re alone. Thus if the values of ϕ taken from the Nikuradze tables are raised to the power $1/\alpha = (2 \ln Re)/3$, and $\phi^{1/\alpha}$ is plotted as a function of η, the result should be a straight line. This is a rigorous test because the power $1/\alpha$ is predetermined and not adjustable. It is also large, of the order of 10, and thus even small deviations from the proposed scaling law should produce a large distortion of the straight line. Figure 5 shows that for all of the 16 series of Nikuradze's experiment, corresponding to Reynolds numbers in the range 4×10^3 to 3.24×10^6 (three

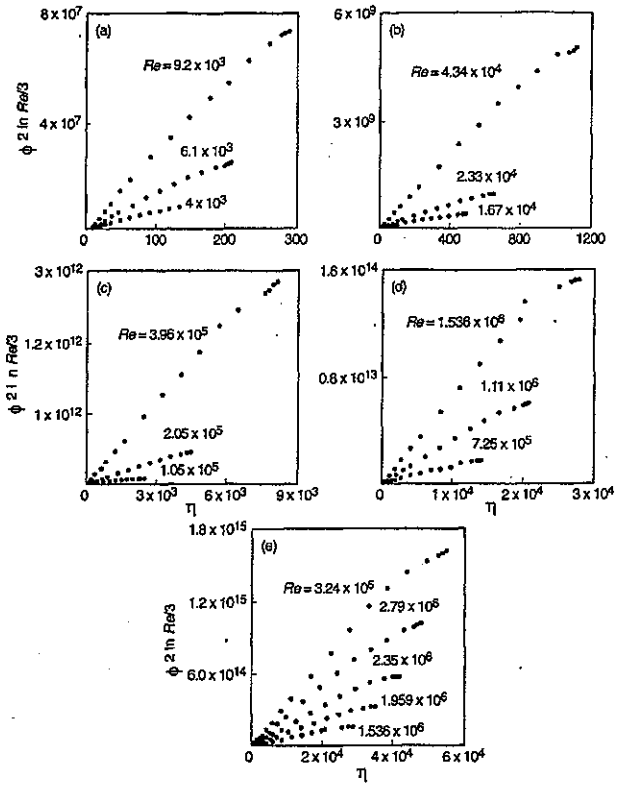

Fig 5. Graphs of $\phi^{(2\ln Re/3)}$ as functions of η reveal straight intervals in the intermediate range of values of η at various Reynolds numbers. These graphs are used to determine the coefficients in the scaling law (1.6).

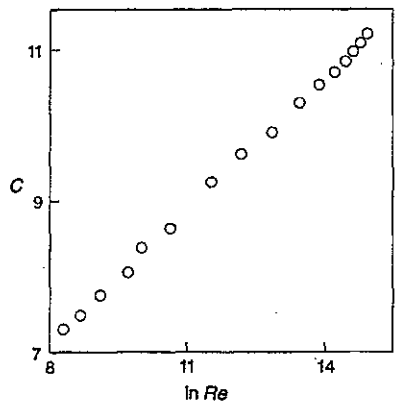

Fig 6. Function C(ln Re) obtained by processing Nikuradze's data

orders of magnitude), the relation between $\phi^{1/\alpha}$ and η was well-represented by a straight line in the intermediate range of values of η.

Step 3. Once the conjectured relation $\alpha_1 = 3/2$ was confirmed, the values of the coefficient $C = C(\mathrm{Re})$ in (4.6) could be found, allowing us to verify the relation $C = C_0 \ln Re + C_1$ and to determine C_0 and C_1. The function $C = C(Re)$ is presented in Fig 6, and is well approximated by the relation

$$C = \frac{1}{\sqrt{3}} \ln Re + \frac{5}{2} \tag{4.8}$$

$\left(C_0 = \frac{1}{\sqrt{3}}, C_1 = 5/2\right)$. In fact, statistical processing has given $C_0 = 0.578 \pm 0.001$, while $\frac{1}{\sqrt{3}} = 0.57735$; the form $\frac{1}{\sqrt{3}}$ simplifies the formulas below. Similarly, the processing of the data yielded $C_1 = 2.50 \pm 0.016$, in the neighborhood of 2.5. Thus the final result is

$$\phi = \left(\frac{1}{\sqrt{3}} \ln Re + \frac{5}{2}\right) \eta^{3/2 \ln Re}, \tag{4.9}$$

or, equivalently,

$$\phi = \left(\frac{\sqrt{3} + 5\alpha}{2\alpha}\right) \eta^{\alpha}, \quad \alpha = \frac{3}{2 \ln Re}. \tag{4.10}$$

Step 4. A further form of (4.9) can be obtained as follows: Introduce the variable ψ,

$$\psi = \frac{1}{\alpha} \ln \frac{2\alpha\phi}{\sqrt{3} + 5\alpha}. \tag{4.11}$$

Equation (4.9) then reduces to

$$\psi = \ln \eta. \tag{4.12}$$

Equation (4.12) is particularly important in what follows. As we have noted at the end of the previous section, a key difference between the universal logarithmic law and the scaling law is that, while the former implies that all the data points in the $(\ln\eta, \phi)$ plane cluster on a single curve, the latter produces one curve $\phi = \phi(\eta)$ per Reynolds number Re, and the corresponding data points should fill out an area in the $(\ln\eta, \phi)$ plane. The transformation (4.11) reverses the roles of the two laws. According to the scaling law, all the data points should cluster in the $(\ln\eta, \psi)$ plane on a single curve, and a particularly simple one at that: the bisectrix of the first quadrant. By contrast, if the universal logarithmic law holds, the data points should be area-filling.

In Fig 7, we plot the experimental data of Nikuradze in the $(\ln\eta, \psi)$ plane. We observe that for $\eta > 25$ (*ie*, outside the viscous sublayer) all the data except for very few fall on the bisectrix, confirming the validity of our scaling law. (A plausible explanation for the four exceptional points as a typographical error has been offered by Professor Coles [personal communication] but we shall not presume to make corrections to the data published by Nikuradze.) For further details on these comparisons, see [7], [9]. It is important to see that Fig 7 also testifies to the self-consistency of the Nikuradze data.

It is also important to compare the prediction of the scaling law (4.9) for the Reynolds number dependence of the drag coefficient with the experimental values. The usual definition of the drag coefficient λ is

$$\lambda = \frac{\tau}{\rho \frac{\overline{u}^2}{8}} = 8\left(\frac{u_*}{\overline{u}}\right)^2. \tag{4.13}$$

The average velocity $\overline{u}$ is given by

$$\overline{u} = \frac{8}{d^2} \int_0^{d/2} u(y) \left(\frac{d}{2} - y\right) dy. \tag{4.14}$$

To calculate $\overline{u}$, we assume that it is possible to replace $u(y)$ in (4.14) by the scaling law (4.9), which is strictly true only in the intermediate region (3) (Fig 1); this introduces a systematic error which should be small at large Re, when the near-wall region 1 and the near-axis region (2) are small. The result is

$$\overline{u} = u_* \frac{\sqrt{3} + 5\alpha}{\alpha} \left(\frac{u_* d}{\nu}\right)^{\alpha} \frac{1}{2^{\alpha}(1+\alpha)(2+\alpha)}. \tag{4.15}$$

From our previous analysis, $Re = \exp(3/2\alpha)$, and therefore

$$\frac{u_* d}{\nu} = \left[\frac{e^{(3/2\alpha)} 2^{\alpha} \alpha (1+\alpha)(2+\alpha)}{\sqrt{3} + 5\alpha}\right]^{1/(1+\alpha)} \tag{4.16}$$

Some further algebra yields an explicit relationship between the dimensionless drag coefficient λ and the Reynolds number Re:

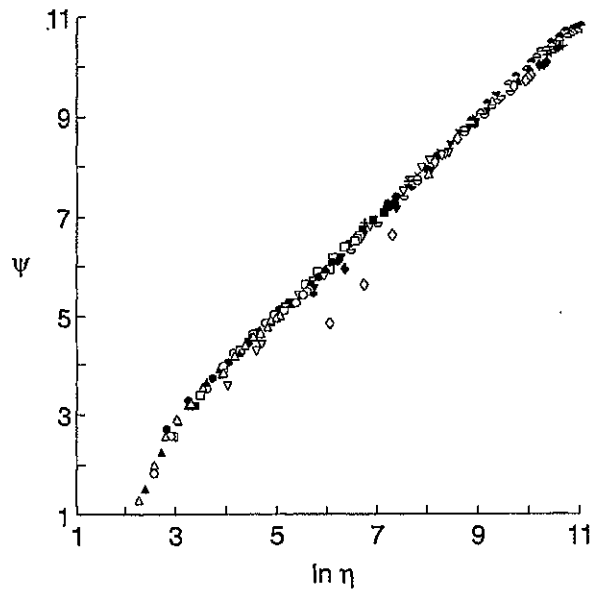

Fig 7. Experimental points in the coordinates $(\ln\eta, \psi)$ at $\eta > 30$ lie close to the bisectrix of the first quadrant, confirming the scaling law (4.9). 1) △, $Re = 4 \cdot 10^3$; 2) ▲ $Re = 6.1 \cdot 10^3$; 3) ○, $Re = 9.2 \cdot 10^3$; 4) •, $Re = 1.67 \cdot 10^4$; 5) ||, $Re = 2.33 \cdot 10^4$; 6) ■, $Re = 4.34 \cdot 10^4$; 7) ▽, $Re = 1.05 \cdot 10^5$; 8) ▼, $Re = 2.05 \cdot 10^5$; 9) ⊍, $Re = 3.96 \cdot 10^5$; 10) ⛊, $Re = 7.25 \cdot 10^5$; 11) ◇, $Re = 1.11 \cdot 10^6$; 12) ◆, $Re = 1.536 \cdot 10^6$; 13) +, $Re = 1.959 \cdot 10^6$; 14) ×, $Re = 2.35 \cdot 10^6$; 15) ⊓, $Re = 2.79 \cdot 10^6$; 16) ⬢, $Re = 3.24 \cdot 10^6$

$$\lambda = \frac{8}{\psi^{2(1+\alpha)}}, \tag{4.17}$$

where

$$\psi = \frac{e^{3/2}\left(\sqrt{3}+5\alpha\right)}{2^{\alpha}\alpha(1+\alpha)(2+\alpha)}, \quad \alpha = \frac{3}{2\ln Re}.$$

The implicit relation between λ and Re, predicated on the logarithmic law, can be found *eg* in [29], page 301, formula (5.45).

In Fig 8 we present the values of the ratio $\xi = \lambda_{exp}/\lambda_{predicted}$ as a function of ln Re for all 125 data points in Nikuradze's paper [31]; λ_{exp} is the experimental value and $\lambda_{predicted}$ is the value given by (4.17) above. Ideally ξ should be equal to one; the difference is within the bounds of experimental error. The very slight systematic deviation may be ascribed to the fact that the scaling law (4.9) is not valid near the wall or near the axis. Figure 9 displays, as a function of ln Re, the following functions: (1) λ as given by (4.17) as a consequence of the scaling law (4.9); (2)λ as given by the *corrected Prandtl law* designed to fit the data [35]; (3) λ as derived from the logarithmic law, using the constants suggested by Zagarola *et al* [38], [39]. The agreement between the first two speaks for itself: No further manipulation of the power law is needed to bring its consequences into line with the experimental data.

5 FURTHER ANALYSIS OF THE SCALING LAW AND OF THE UNIVERSAL LOGARITHMIC LAW

Our proposed scaling law can be written in the form

$$\phi = \left(\frac{1}{\sqrt{3}}\ln Re + \frac{5}{2}\right)\exp\left(\frac{3\ln\eta}{2\ln Re}\right), \tag{5.1}$$

clearly revealing the self-similarity property of the scaling law curves in the (lnη, ϕ) plane: The curves (5.1) can be obtained from each other by similarity transformations; in the reduced variables $X = \frac{3\ln\eta}{2\ln Re}, Y = \phi\left(\frac{1}{\sqrt{3}}\ln Re + \frac{5}{2}\right)^{-1}$ all the scaling law curves collapse on a single curve. For each value of Re we obtain a distinct curve $\phi = \phi(\eta)$, in contrast to the prediction of the universal logarithmic law, according to which all the data points should lie on a single curve in the (lnη, ϕ) plane. The envelope of the family of curves (5.1), with parameter Re, is obtained by eliminating Re between (5.1) and the condition $\partial_{\ln Re}\phi = 0$; the last equation can be written as

$$\frac{3\ln\eta}{2\ln Re} = \frac{\sqrt{3}}{10}(\ln\eta)\left[\left(1+\frac{20}{\sqrt{3}\ln\eta}\right)^{1/2} - 1\right]. \tag{5.2}$$

This envelope is shown in Fig 10, together with the straight line $\phi = 2.5\ln\eta + 5.5$, given by Schlichting [35] as the universal logarithmic law. It is clear that these two

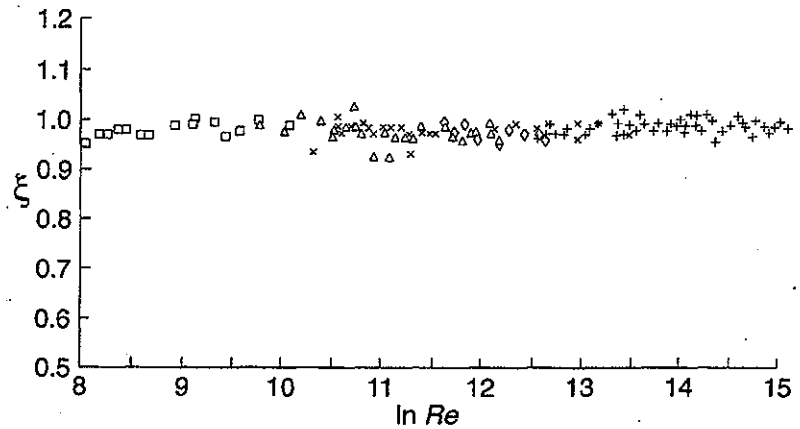

Fig 8. Nikuradze data for various pipes and various Reynolds numbers confirm with good accuracy the friction law (4.17) which follows from the scaling law (4.9); the figure shows $\xi = \lambda_{exp}/\lambda_{predicted}$ for various pipes: ⁞, d = 1 cm; Δ, d = 2 cm; ◇, d = 3 cm; ×, d = 5 cm; +, d = 10 cm

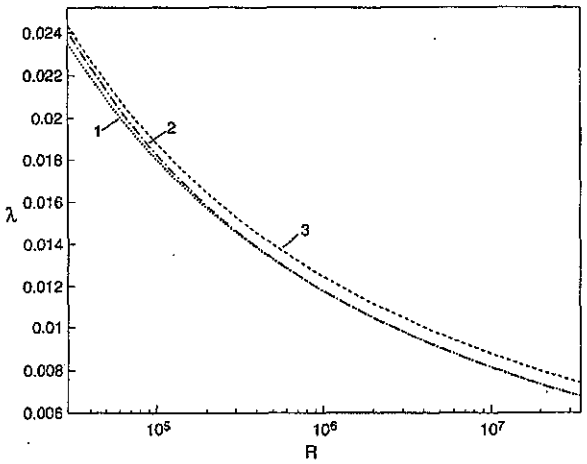

Fig 9. Friction parameter λ as a function of ln Re, obtained as follows: 1) λ as given by (4.17) as a consequence of the power law; 2) λ as given by the "corrected Prandtl law" designed to fit the data [35]; and 3) λ as derived from the logarithmic law, using the constants $\kappa = 0.44$, $B = 6.3$ suggested by the Princeton group [38].

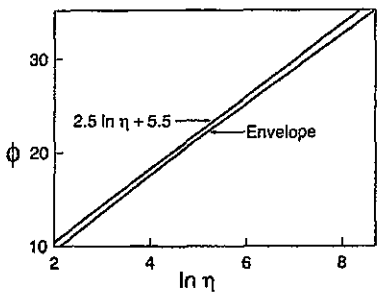

Fig 10. The envelope of the scaling law curves in the (lnη, ϕ)-plane is very close to the generally accepted straight line of the universal logarithmic law, even at moderate η.

curves are close in the range of η under consideration. If the constant 5.5 is replaced by 5.1 the two curves practically coincide. Indeed, the line $\phi = 2.5 \ln \eta + 5.1$ is the universal logarithmic law as quoted in Monin and Yaglom [29].

If one allows $\ln Re \to \infty$, $\ln\eta \to \infty$ while remaining on the envelope, the coefficients in the equation of the envelope tend to a finite limit, such that

$$\phi = \frac{\sqrt{3e}}{2}\ln\eta + \frac{5}{2}e + \text{ small quantities.} \tag{5.3}$$

The value $\left(\frac{\sqrt{3e}}{2}\right)^{-1} \cong .425$ is close to the value of von Kármán's constant $\kappa = .417$ obtained by Nikuradze. However, the value of the additive constant $\frac{5}{2}e \cong 6.79$ is substantially larger than the values commonly ascribed to the additive constant B in the logarithmic law (1.7). For this asymptotic value to be observed the values of $\ln \eta$ and $\ln Re$ have to be large enough for two things to happen simultaneously: The asymptotic regime must be reached on the asymptote while the asymptote still approximates the individual curves (see below). Apparently, velocity profiles at small enough values of ν and close enough to the wall have not been measured in experiments with pipe flow.

Figure 11 presents three of Nikuradze's experimental runs, with Reynolds numbers differing approximately by an order of magnitude: $Re = 1.67 \times 10^4$, $Re = 2.05 \times 10^5$, $Re = 3.24 \times 10^6$. The corresponding scaling curves (4.9), the straight line of the universal logarithmic law, and the envelope of the family of scaling law curves are also exhibited. It can be seen that the scaling law curves have a small systematic and discernible advantage over the logarithmic law. At this stage, we do not wish to emphasize this advantage, and indeed, we would like to point out that all of Nikuradze's data correspond to points near the envelope of the scaling law curves. We shall later present far more decisive criteria for deciding between the logarithmic and scaling laws.

Having fitted constants to the scaling law from the available data, which are close to the envelope, we shall now extrapolate the resulting law to points farther from the envelope, taking care not to alter the constants. If the constants are universal, they should be the same for all data points from all experiments whose quality matches that of Nikuradze's experiments. If the extrapolation is successful in predicting the data, the result is a dramatic validation of the scaling law. The extrapolation will be carried out with the help of vanishing-viscosity asymptotics, based on the hypothesis that a vanishing-viscosity limit exists, as explained above.

Consider again the scaling law, equation (4.9). If one stands at a fixed distance from the wall, in a specific pipe with a given pressure gradient, one is not free to vary $Re = \overline{u}d/\nu$ and $\eta = u_*y/\nu$ independently because the viscosity ν appears in both, and if ν is decreased by the experimenter, the two quantities will increase in a self-consistent way. The limit of the velocity gradient that corresponds to the experimental situation is the limit of vanishing viscosity. The existence of this limit has already been asserted. When one takes the limit of vanishing viscosity, one considers flows at ever larger η at ever larger Re; the ratio $\frac{3\ln\eta}{2\ln Re}$ tends to 3/2 because ν appears in the same way in both numerator and denominator. Indeed, consider the combination $3\ln\eta/2\ln Re$. It can be represented in the form

$$\frac{3\ln\eta}{2\ln Re} = \frac{3\left[\ln\frac{u_*d}{\nu} + \ln\frac{y}{d}\right]}{2\left[\ln\frac{u_*d}{\nu} + \ln\frac{\overline{u}}{u_*}\right]}. \tag{5.4}$$

According to (4.15), at small ν, *ie* large Re, $\overline{u}/u_* \sim \ln Re$, so that the term $(\overline{u}/u_*)$ in the denominator of the right-hand side of (4.9) is asymptotically small, of the order of $\ln\ln Re$, and can be neglected at large Re. The crucial point is that due to the small value of the viscosity ν the first term $\ln(u_*d/\nu)$ in both the numerator and denominator of (5.4) should be dominant, as long as the ratio y/d remains bounded from below, for example by a predetermined fraction. Thus, as long as one stays away from a suitable neighborhood of the wall, the ratio $3\ln\eta/2\ln Re$ is close to 3/2 (y is obviously bounded by $d/2$). Therefore the quantity

$$1 - \ln\eta / \ln Re$$

can be considered as a small parameter, as long as $y > \Delta$, where Δ is an appropriate fraction of d. The quantity $\exp(3\ln\eta/2\ln Re)$ is approximately equal to

$$\exp\left[\frac{3}{2} - \frac{3}{2}\left(1 - \frac{\ln\eta}{\ln Re}\right)\right] \approx e^{3/2}\left[1 - \frac{3}{2}\left(1 - \frac{\ln\eta}{\ln Re}\right)\right] = e^{3/2}\left[\frac{3}{2}\frac{\ln\eta}{\ln Re} - \frac{1}{2}\right]. \tag{5.5}$$

According to (4.9) we have also

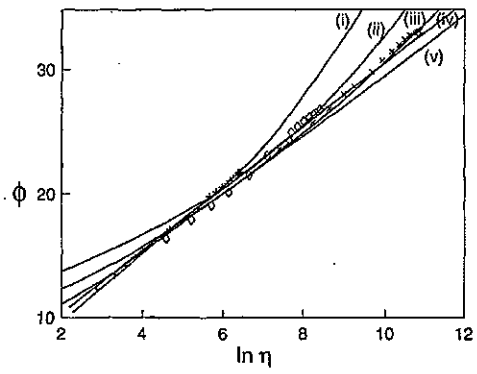

Fig 11. Experimental points and the scaling law curves at various Reynolds numbers: *i*) (+, $Re = 1.67 \cdot 10^4$), *ii*) (◇, $Re = 2.05 \cdot 10^5$), *iii*) (×, $Re = 3.24 \cdot 10^6$), *iv*) universal logarithmic law, and *v*) envelope

$$\eta\partial_\eta\phi = \partial_{\ln\eta}\phi = \left(\frac{\sqrt{3}}{2} + \frac{15}{4\ln Re}\right)\exp\left(\frac{3\ln\eta}{2\ln Re}\right), \qquad (5.6)$$

and the approximation (5.5) can also be used in (5.6). Thus in the intermediate asymptotic range of distances y: $y > \Delta$, but at the same time y slightly less than $d/2$, the following asymptotic relations should hold as $Re \to \infty$

$$\phi = e^{3/2}\left(\frac{\sqrt{3}}{2} + \frac{15}{4\ln Re}\right)\ln\eta - \frac{e^{3/2}}{2\sqrt{3}}\ln Re - \frac{5}{4}e^{3/2}, \qquad (5.7)$$

and

$$\partial_{\ln\eta}\phi = \frac{\sqrt{3}}{2}e^{3/2}. \qquad (5.8)$$

At the same time it can be easily shown that for the envelope of the power-law curves the asymptotic relation is

$$\partial_{\ln\eta}\phi = \frac{\sqrt{3}}{2}e. \qquad (5.9)$$

The difference in slopes between (5.8) and (5.9) is significant. It shows that individual members of the family (4.9) should have at large Re an intermediate part, represented in the plane ($\ln\eta$, ϕ) by straight lines, with a slope different from the slope of the envelope by a factor $\sqrt{e} \sim 1.65$. Therefore the graph of the individual members of the family (4.9) should have the form presented schematically in Fig 12.

We now examine in detail a well-known argument for determining the structure of the flow in the region intermediate between the immediate vicinity of the wall and the region far from the wall. This argument is due to Izakson, Millikan and von Mises (IMM) (see *eg* [18], [29]). In this argument, it is assumed that from the wall outward, for some distance, one has a generalized law of the wall,

$$\phi = u/u_* = f(u_* y/\nu) \qquad (5.10)$$

where f is a dimensionless function; the influence of the Reynolds number Re, which contains the external length scale (for pipe flow, the diameter d of the pipe) is neglected; heuristically, it is assumed that fluid near enough to a smooth wall does not feel the outer part of the flow. Adjacent to the axis of the pipe in pipe flow and extending to the sides one assumes a *defect law*,

$$u_{CL} - u = u_* g(2y/d), \qquad (5.11)$$

where u_{CL} is the average velocity at the centerline and g is another dimensionless function. Here the neglect of the effect of Re means that the effect of viscosity is neglected; heuristically, one assumes that near the axis, where the velocity gradients are small, the effect of a small enough viscosity is unimportant. Both assumptions taken together constitute an assumption of *separation of scales*, according to which at large enough yet finite values of Re viscous scales and inviscid scales can be studied in partial isolation. Self-consistency then demands that for some interval in y the laws (5.10) and (5.11) overlap, so that

$$u_{CL} - u = u_{CL} - u_* f(u_* y/\nu) = u_* g(2y/d). \qquad (5.12)$$

After differentiation of (5.12) with respect to y followed by multiplication by y, one obtains

$$\eta f'(\eta) = -\xi g'(\xi) = \frac{1}{\kappa}, \qquad (5.13)$$

where $\eta = u_* y/\nu$, $\xi = 2y/d$, and κ is a constant; integration then yields the law of the wall

$$f(\eta) = \frac{1}{\kappa}\ln\eta + B, \qquad (5.14)$$

as well as the defect law

$$g(\xi) = -\frac{1}{\kappa}\ln\xi + B_*, \qquad (5.15)$$

with

$$B_* = \frac{u_{CL}}{u_*} - \frac{1}{\kappa}\ln\frac{u_* d}{2\nu} - B.$$

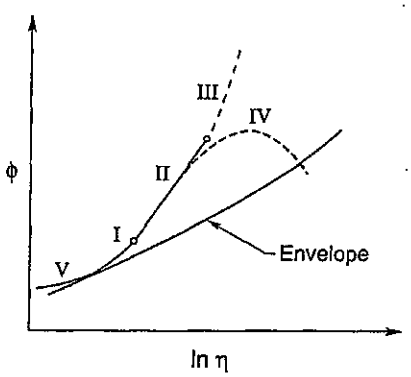

Fig 12. The individual members of the family of scaling laws (4.9) near the envelope in the ϕ, $\ln\eta$-plane have a straight intermediate interval with a slope substantially larger than that of the envelope: I) Part close to the envelope; II) Straight intermediate part; III) Fast growing ultimate part having no physical meaning because there are no corresponding points in the pipe; IV) Region near the axis of the pipe where the scaling law is invalid; V) Part which was never observed because of the large diameter of the gauge.

However, the experimental data (see *eg* Fig 7 in [38]) do not support the assumption of separation of scales. We now examine what happens if one repeats the elegant but oversimplified argument we have just described without dropping the effects of Re near the wall and near the center of the pipe. We shall see that, when properly improved, the argument survives and supports our conclusions.

We begin by noting that in the nearly linear portion II of the graph of Fig 12 the flow can be described by a local logarithmic law with a Reynolds number dependent effective von Kármán constant $\kappa_{eff} = \kappa(Re)$:

$$\kappa_{eff} = \frac{2}{\sqrt{3}e^{3/2} + \ldots}; \qquad (5.16)$$

as $Re \to \infty$, $\kappa(Re)$ tends to the limit $\kappa_\infty = \frac{2}{\sqrt{3}e^{3/2}} \sim 0.2776\ldots$, smaller than the usual von Kármán constant $\kappa = \frac{2}{\sqrt{3}e} \sim .425\ldots$ by a factor $\sqrt{e} \sim 1.65\ldots$. With this in

mind, the IMM procedure can be modified as follows: The law of the wall, equation (5.10), becomes

$$\phi = u/u_* = f(u_* y/\nu, Re) \tag{5.17}$$

so that the influence of Re, which contains the external scale, is included. The previous defect law (3.2) is also replaced by the Reynolds number dependent defect law

$$u_{CL} - u = u_* g(2y/d, Re), \tag{5.18}$$

so that the influence of the molecular viscosity ν is preserved. Now assume that the laws (5.17) and (5.18) overlap on some y interval:

$$u_{CL} - u = u_{CL} - u_* f(u_* y/\nu, Re) = u_* g(2y/d, Re).$$

Replacing f by its expression (5.7) yields:

$$g(2y/d, Re) = \phi_{CL} - \left(\frac{1}{\sqrt{3}}\ln Re + \frac{5}{2}\right)e^{3/2} - \left(\frac{\sqrt{3}}{2} + \frac{15}{4\ln Re}\right)e^{3/2}\ln(2y/d) - e^{3/2}\left(\frac{\sqrt{3}}{2} + \frac{15}{4\ln Re}\right)\ln\frac{u_*}{2\bar{u}}, \tag{5.19}$$

where $\phi_{CL} = u_{CL}/u_*$. This calculation is self-consistent, and differs from the original IMM procedure by matching a Reynolds number dependent defect law to the actual curves of the scaling law (4.9) rather than to their envelope misinterpreted as being identical to the actual curves.

Another way of looking at the calculation we have just performed is to note that if one requires an overlap between a law of the wall that does not depend on d and a defect law that does not depend on ν, one obtains an overlap that depends on neither d nor ν; this enforces complete similarity and results in the von Kármán-Prandtl law, which can be obtained by simply removing the quantities d and ν from the list of arguments in equation (1.8). On the other hand, more realistic requirements on the laws being matched leave room for incomplete similarity and are consistent with the scaling law (4.9) and with the experimental data; for example, Fig 7 in [38] exhibits clearly the dependence of the profile in the neighborhood of the centerline on ν. The matching was successfully carried out because the scaling law has an intermediate range that is approximately linear in $ln\eta$; the success of the matching does not depend on the specific values of the constants C_0, C_1 and α_1 in (4.9).

Note also that the inner and outer portions of the flow *feel* each other for all finite values of Re; the coupling disappears only in the limit of vanishing viscosity. Note further that as the viscosity is decreased beyond the point where the *chevron* appears, the location of the kink in the chevron moves slowly towards the wall; at extremely high Reynolds numbers, well beyond those currently achieved in the laboratory, the power law collapses onto the upper part of the chevron, resulting in an apparent new logarithmic law, with constants different from the usual constants in the von Kármán-Prandtl law; in particular the new value of the *von Kármán constant* would be, as shown above, $\kappa_\infty = \frac{2}{\sqrt{3}e^{3/2}} \sim 0.2776$. It is important to remember that this new logarithmic law, corresponding to the upper part of the chevron, lies in the area of *deviation* in Fig 2 and 3 and not where the usual von Kármán -Prandtl is usually placed.

6 FURTHER COMPARISON OF THE SCALING LAW WITH THE EXPERIMENTAL DATA

The dramatic feature of the velocity profile in the $(\ln\eta,\phi)$ plane at a small viscosity ν, predicted in the previous section, is its chevron (broken line) form: The limits $\nu \to 0$ of the scaling law curves have a kink where they leave the envelope, and the difference in the slopes of the two branches of the chevron is substantial, more than $\sqrt{e} \sim 1.65$.

There exist many confirmations of this behavior, both in old and in new experiments. A few examples should suffice: the experimental data of Schubauer and Klebanoff [29], (the full squares in Fig 3), the 1951 experimental data of Wieghardt and Tilliman [36], (Fig 13), and the particularly instructive data presented by Fernholz and Finley in 1995

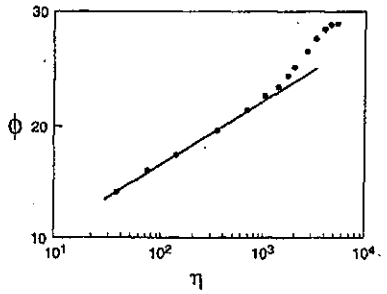

Fig 13. Data of Wieghardt and Tilliman (see [37]) obtained in a boundary layer flow confirm the chevron-like velocity distribution in the (ln η, ϕ) plane predicted in Fig 12

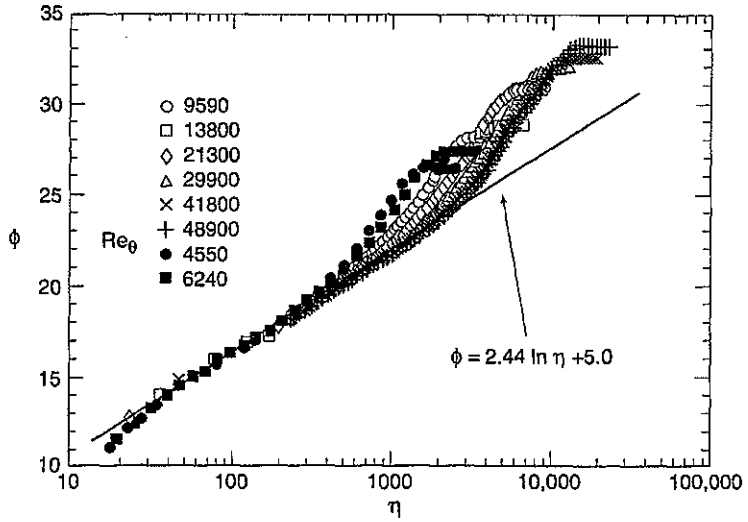

Fig 14. Data of Nagib and Hites [23], [30] obtained in a floor boundary layer flow. (Reproduced with permission from [30])

([19], see in particular their Fig 28 - 30) and by Nagib and Hites [23], [30] in 1995 (see Fig 14). The chevron structure of the flow was not properly understood at the time when these data were published, and the upper branch was attributed either to the nature of the external flow or to experimental scatter. However, all these data were for boundary layer flows rather than for pipe flow, and thus have additional features which we shall discuss elsewhere.

Recently there appeared an experimental study from the Princeton group of Zagarola *et al* [38], [39] with many new data points for pipe flow, obtained in the high-pressure pipe (superpipe) proposed by Brown [12]. High pressure increases the density ρ, and increases the dynamic viscosity μ at a much smaller rate, decreasing the kinematic viscosity $\nu = \mu/\rho$ substantially and thus increasing the Reynolds number *Re*. It was claimed that in this way one can increase the Reynolds number by an order of magnitude over the *Re* achieved by Nikuradze with a flow of water.

It is shown, later in this section, that for Reynolds number $Re > 10^6$, the Princeton data contain a systematic error. Nevertheless, as one can clearly see from Fig 15 reproduced with permission from [38], the appearance of a chevron structure and the splitting of the velocity curves according to their Reynolds number are so strong that even a systematic error at large *Re* cannot destroy them. To each *Re* corresponds its own curve in the $(\ln\eta,\phi)$ plane, with a pronounced linear part whose slope is larger than the slope of the envelope by a factor that is always larger than 1.5. For smaller values of y the deviation of the curves from their envelope is small (corresponding to part I of the curve in Fig 13).

We consider this graph to be a clear confirmation of the proposed scaling law, and as a strong argument against the universal logarithmic law.

We emphasize the important consequences of our vanishing-viscosity analysis of the scaling law curves and of the

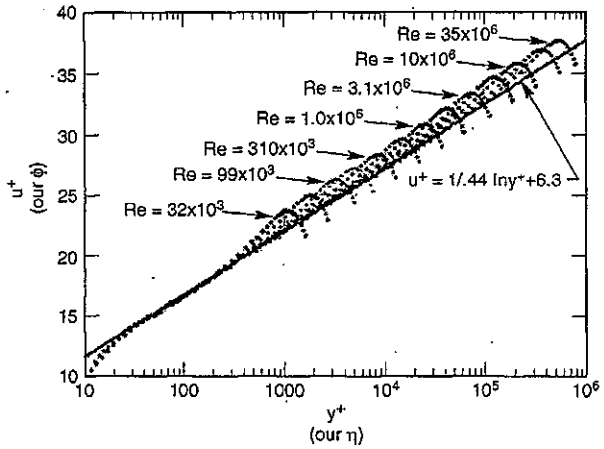

Fig 15. Princeton data [38] obtained in a high-pressure pipe confirm the splitting of the experimental data according to their Reynolds numbers and the predicted chevron-like velocity distribution in the $(\ln\eta, \phi)$-plane. The splitting and chevron-like form of the velocity profile agree with the scaling law, and are incompatible with the universal logarithmic law. (Reproduced with permission from [38]).

experimental data:

(i) Both linear parts of the piecewise linear chevron structure belong to the same scaling law; the constants that describe the inner (*ie* closer to the wall) segment also describe the outer segment.

(ii) The overlap region is the outer segment of the chevron; thus the outer segment belongs both to the wall region and to the defect region.

(iii) There is no other possible locus for the overlap; as the slopes of the outer and the inner segments tend to two different constants as $\nu \to 0$, one can never get them to overlap on the inner segment.

(iv) The whole chevron constituting a single law, the possibility that the inner segment is described by the universal (*ie Re* independent) logarithmic law is excluded.

(v) More generally, since the defect law must be a concave-downward function of y/d, the only way there can ever be a portion of the velocity profile that is concave upwards outside the near vicinity of the wall, as observed in Fig 15, is to make the overlap region be concave upward, as we are proposing, rather than straight.

We note that the prediction of a difference $\sqrt{e}$ between the slopes of the individual velocity profiles and the slope of their envelope provides an easily verified criterion for assessing the agreement between the experimental data and the scaling law. At high *Re* the difference between the proposed scaling law and the universal logarithmic law is large enough to have a substantial impact on the outcome of engineering calculations.

Now we come to more detailed comparison of the proposed scaling law with the data presented by the Princeton group. The advantage of this set of data for such comparisons is that, like the data of Nikuradze, they are presented in tabular form. The Princeton group presented results of 26 runs (series of experiments), each run containing the data from measurements of the velocity distribution over the cross-section of the pipe, as well as the measured drag coefficients. The experiments were performed with air flow in a pipe at high pressure (the pressure varied from ~ 1 to ~ 190 atmospheres). The kinematic viscosity of air under normal conditions is ~ 0.15cm^2/s, that of water is ~ 0.01cm^2/s, therefore the Princeton group had to compress the air to roughly 15 atmospheres to reach the kinematic viscosity of water. As we will see later, it is at this point that the Princeton experiments became inaccurate.

Another important advantage of the Princeton data is that they contain many experimental points far from the envelope (see Fig 15). In the published experiments of Nikuradze there were no such data. Therefore the most interesting step is the comparison of the Princeton data with the scaling law (4.9) according to the same procedure as in section 4. Thus all the Princeton data were plotted in the $(\ln\eta, \psi)$ plane, where, as before,

$$\psi = \frac{1}{\alpha}\ln\frac{2\alpha\phi}{\sqrt{3+5\alpha}}, \quad \alpha = \frac{3}{2\ln Re}, \quad Re = \frac{\overline{u}d}{\nu} \quad \phi = \frac{u}{u_*}. \quad (6.1)$$

For the first ten runs ($Re = 3.16 \cdot 10^4$, $4.17 \cdot 10^4$, $5.67 \cdot 10^4$, $7.43 \cdot 10^4$, $9.88 \cdot 10^4$, $1.46 \cdot 10^5$, $1.85 \cdot 10^5$, $2.30 \cdot 10^5$,

$3.09 \cdot 10^5$, $4.09 \cdot 10^5$), the data are presented in Fig 16. It is seen that as in the case of the Nikuradze data, the experimental points after $\eta = 25$ concentrate near the bisectrix of the first quadrant, as they should according to the model presented above. The points close to the pipe axis should be removed because the scaling law should be invalid for them. It was enough to remove only the points where $2y/d$ was more than 0.95.

However, for the last six runs (Re = $1.02 \cdot 10^7$, $1.36 \cdot 10^7$, $1.82 \cdot 10^7$, $2.40 \cdot 10^7$, $2.99 \cdot 10^7$, $3.52 \cdot 10^7$) the situation is different: the experimental points for all these runs are concentrated (for $y/R < 0.95$, $R = d/2$) along straight lines, parallel to the bisectrix, but not on the bisectrix itself (Fig 17). Note that all these curves present a chevron, and there is a separate curve for each value of Re; the advantage of the scaling law over the universal logarithmic law is not in question even in the presence of this disturbing shift in the processed curves.

Some hint to what happens was given by a comparison of the experiments of Nikuradze and of the Princeton group performed at roughly equal Reynolds numbers. There are six such experiments, and for five of them, at moderate Reynolds numbers, a satisfactory coincidence was found. This coincidence means that our scaling law (4.9) is also confirmed by the Princeton experiments. However, for the Princeton run #16 with $Re = 2.345 \cdot 10^6$, and the corresponding run of Nikuradze ($Re = 2.35 \cdot 10^6$), which, like the other Nikuradze runs, corresponds quite satisfactorily to our model, a noticeable disagreement was found (Fig 18). In the main part of the graph in the ($\ln\eta$, ϕ)-plane there is a nearly uniform shift along the $\ln\eta$ axis. What can be the meaning of such a shift? If both u_* and y were measured correctly, the most likely source of the discrepancy is in the determination of the viscosity. It is of importance that the pressure gradients in these experiments are small enough not to create a variation of the viscosity along the pipe, and thus in each run the viscosity can be viewed as constant.

We concluded that something happened in the high Reynolds number-high pressure Princeton experiments which

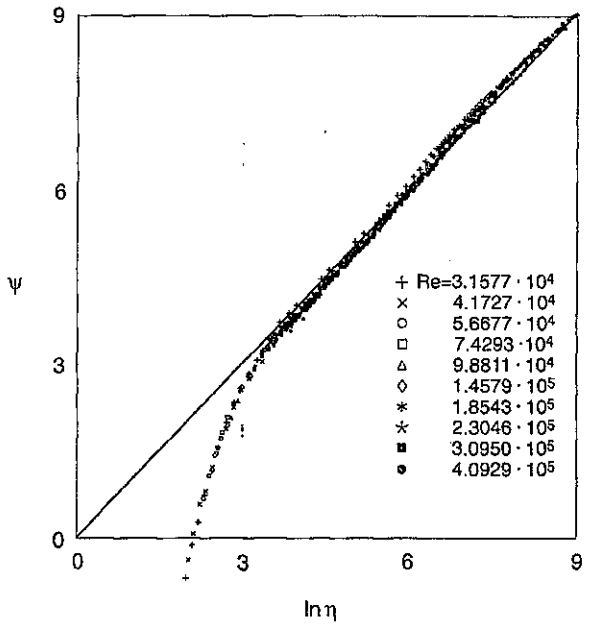

Fig 16. The lower Reynolds number Princeton data [39] are in agreement with the scaling law: In the (ln η, ψ) plane they are close to the bisectrix (except, as it should be, in the near-axis region).

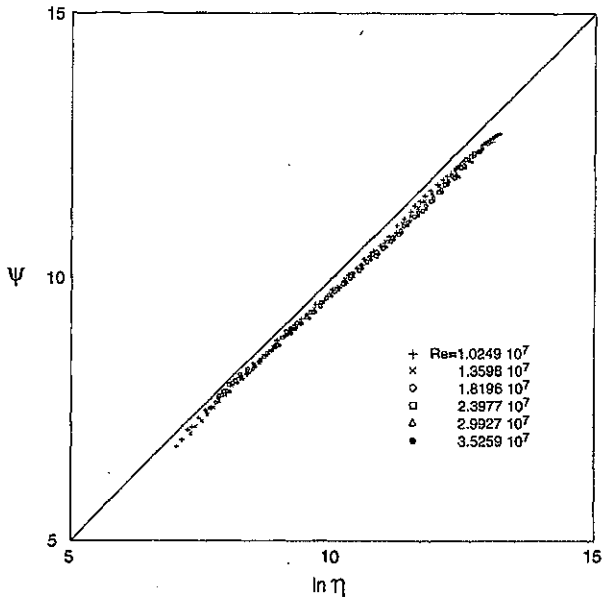

Fig 17. There is a noticeable disagreement between the large Reynolds numbers Princeton data and the prediction of the scaling law (4.9): In the (ln η, ψ) plane they concentrate along lines parallel to the bisectrix, not on the bisectrix itself. The points with $2y/d > 0.95$ are excluded; they are in the near-axis region.

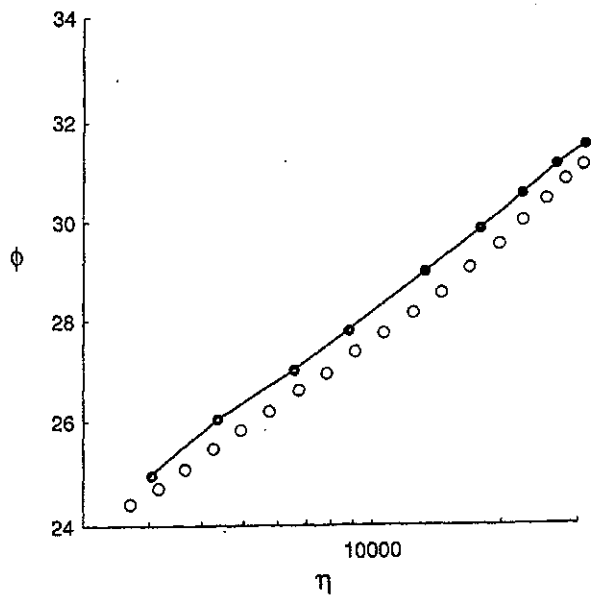

Fig 18. There is disagreement between the Princeton data at $Re = 2.345 \cdot 10^6$ and Nikuradze's data at $Re = 2.35 \cdot 10^6$.

shifted the viscosity that determines the velocity profile from its actual value ν to a *shifted*, effective value ν', so that

$$\ln\eta = \ln\frac{u_* y}{\nu} = \ln\frac{u_* y}{\nu'} + \ln\frac{\nu'}{\nu} \tag{6.2}$$

and the shift $\ln(\nu'/\nu)$ is constant for each run.

To check this conclusion, the following procedure was used for the last six runs. For every experimental point of each run, the value of difference

$$\chi = \ln\eta - \psi \tag{6.3}$$

and $\overline{\chi}$, the mean value of χ per run, were calculated. The dispersion of this quantity was also calculated and found to be very small. Then every experimental point was shifted by $\overline{\chi}$ inwards along the $\ln\eta$ axis. The results are presented in Fig 17 (unshifted points), and Fig 19 (after the shift). They show that there exists a single factor per run by which the viscosity is altered and shifts the velocity profiles at high Reynolds numbers; this does not happen at moderate Reynolds numbers.

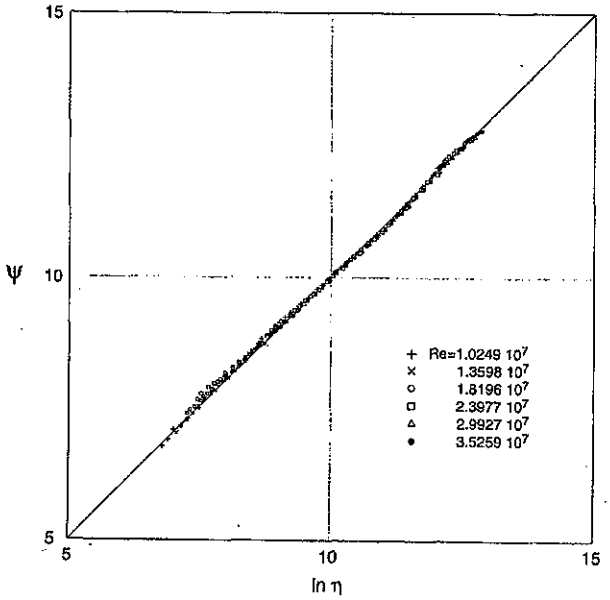

Fig 19. After the viscosity correction (constant for each run), the large Reynolds numbers Princeton data agree with the prediction of the scaling law in the ($\ln\eta$, ψ) plane; the points are close to the bisectrix (except for the near-axis points).

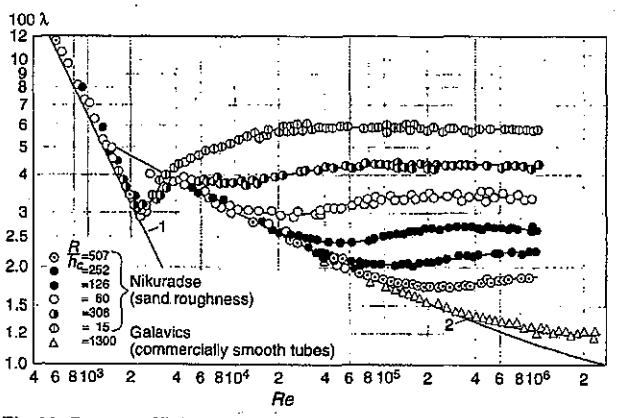

Fig 20. Drag coefficient λ as a function of the Reynolds number for pipes of various roughness (after Monin and Yaglom [29]). (1) Laminar flow, (2) law for smooth pipes.

Three possible reasons were investigated.

(i) Incorrect pressure or temperature measurement. The density and viscosity were not measured directly, but were calculated by the Princeton group on the basis of the measured pressures and temperatures. Therefore an incorrect pressure measurement could be the reason for the "shift" (the measurement of the temperature was not in doubt). After an inspection of the information presented in the thesis [39] we came to the conclusion that this was unlikely.

(ii) Incorrect density and viscosity calculations. Indeed, the Princeton group used rather old pressure-density relations for their calculations. We asked Dr Friend (National Institute of Standards and Technology) to supply us with the values of the density and viscosity of air at the pressures and temperatures recorded in [39]. The data of Friend [20] confirmed the Princeton group's calculations very accurately.

This confirmation has left only one possible explanation for the observed shift in the viscosity. As is well known, if the walls of the pipe are not sufficiently smooth, the roughness protrudes from the viscous sublayer, and a shift in the velocity profile is observed in the intermediate region, exactly as if the viscosity of fluid were changed. There is a well known formula for the equivalent viscosity (see *eg* Monin and Yaglom [29], p 286, formula (5.25b)). Therefore, the last possible reason for the shift is:

(iii) The roughness of the pipe walls is revealed at large Reynolds numbers. To check this possibility we turn to well-known data concerning the Reynolds number dependence of the drag coefficient for flows in rough pipes (see Fig 20,

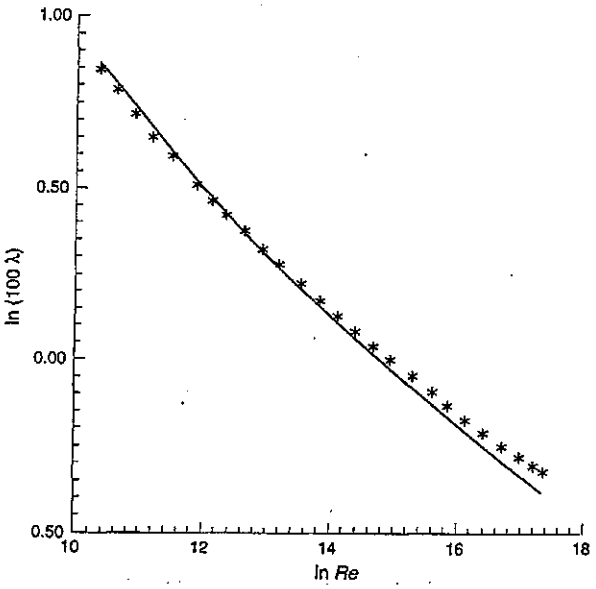

Fig 21. Drag coefficient λ as a function of the Reynolds number for the Princeton data. *- Princeton data; the continuous line is the law for smooth pipes.

available, *eg* in Monin and Yaglom [29] p 308). The general situation is as follows. For a given mean height of the roughness the data for smooth and rough pipes coincide, up to a critical Reynolds number. When this is reached the Reynolds number dependence of the drag coefficient for rough pipes deviates from that for smooth pipes. Clearly the critical Reynolds number depends on the mean height of the roughness: the lesser the height, the later the deviation begins.

The analog of Fig 20 for the Princeton experiments is presented in our Fig 21; the solid line corresponds to the theoretical relation (4.17). The graph shows that the deviation starts approximately at $Re = 10^6$. This is a sensitive indicator of the quality of the velocity profiles; it shows that starting from run 13 ($Re = 1.02 \cdot 10^6$) the profiles presented by the Princeton group are inappropriate for comparison with theoretical predictions for smooth pipes, and that this is the reason for the observed differences between predicted profiles and the profiles measured by the Princeton group.

An even sharper visualization of the effect of roughness on the Princeton data is offered in Fig 22, where the relative friction coefficient $\xi = \lambda_{exp}/\lambda_{predicted}$, (already used in Fig 8 above), calculated from these data is plotted as a function of ln *Re*. One can see that starting approximately from $Re = 10^6$ (ln $Re \sim 13.8$) the values of ξ begin to grow steeply (compare with Fig 8 where nothing happened at this value of *Re*). If the same viscosity correction as the one used in Fig 19 is introduced into the calculation of $\lambda_{predicted}$, the kink disappears, as one can see in Fig 23, where $\xi = \lambda_{exp}/\lambda_{corrected}$ is plotted. This shows that starting with $Re = 10^6$ the drag estimate based on the assumption that the pipe is smooth becomes increasingly insufficient.

As we see, the procedure proposed in section 4 was sensitive enough to detect the disagreement between the Princeton experimental results and theoretical predictions for velocity profiles in smooth pipes, which starts at the point where the roughness comes out of the viscous sublayer according to the drag coefficient data.

Moreover, consider the kinematic viscosity of air in the last run which corresponds to a smooth pipe. According to the Princeton data it can be estimated as approximately $1.05 \cdot 10^{-2} cm^2/s$ – equal to the kinematic viscosity of water.

We come to the conclusion that the Princeton group did not surpass the range of Reynolds number achieved by Nikuradze or reach its upper bound. It is possible that this problem could be cured in a large-pipe experiment, as proposed by Hussain [24].

All the new data support the scaling law over the logarithmic law, and for the lower and intermediate ranges of Reynolds numbers also support the power law with the specific constants we have derived from the Nikuradze data. The data at higher Reynolds numbers are not reliable, and no quantitative conclusions can be drawn from them.

As was noted by Hussain, in addition to the problems with roughness there are the additional issues of the size of the sensor, which can have a significant averaging effect, and the length of the superpipe, which may be too short to allow a full development of the flow. The required length may well depend on *Re*.

7 CONCLUSION

We have shown that the von Kármán-Prandtl universal logarithmic law for the intermediate region of wall-bounded shear flow must be jettisoned and replaced by a power law, of which we have offered a specific form that agrees with the data. In particular, the friction coefficient can be derived from our power law without any further ad-hoc manipulations.

It is interesting to discover what physical mechanisms are responsible for producing a power law. We shall now briefly

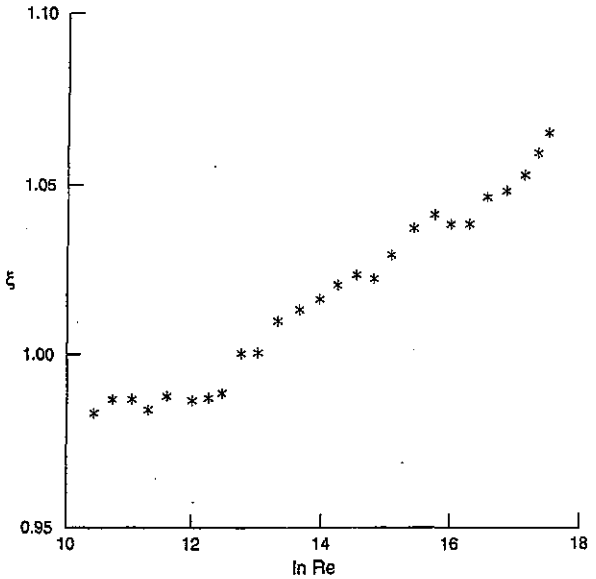

Fig 22. Relative friction $\xi = \lambda_{exp}/\lambda_{predicted}$ for the Princeton data as a function of ln *Re*

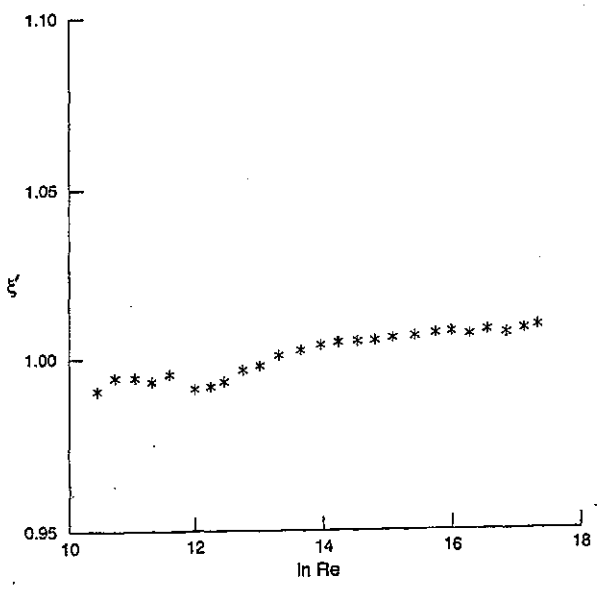

Fig 23. The relative friction $\xi' = \lambda_{exp}/\lambda_{corrected}$ with corrected viscosity as in Fig 19 does not exhibit a kink at $Re \sim 10^6$.

show that the scaling law (4.9) arises because the vorticity in the pipe is intermittent; this intermittency, associated with the vorticity bursting process, is well-documented in the experimental and numerical literature [10], [27], [36], [37].

Indeed, a natural measure of the length scale of the cross-section of the transverse vortical structures near the wall, which are responsible for the vertical variation in the velocity u, is $\ell = (\partial_y u/u_*)^{-1}$; The scaling law (4.9) gives

$$\ell = \frac{2}{\sqrt{3}+5\alpha} y^{1-\alpha} \left(\nu / u_*\right)^{\alpha}, \quad \alpha = \frac{3}{2\ln Re}. \tag{7.1}$$

Note that ℓ is proportional to $y^{1-\alpha}$ rather than to y, showing that the transverse vortical structures are not space filling if (4.9) holds; the universal logarithmic law, on the other hand, produces an ℓ proportional to y. In a viscous flow the vorticity can presumably vanish only on smooth surfaces, but one can define an essential support of the vorticity, (see [14]), as the region where the absolute value of the vorticity exceeds some predetermined threshold; according to (7.1), the intersection of that essential support with a vertical line has fractal dimension $1-\alpha$. If the essential support is statistically invariant under translations parallel to the wall, the essential support itself has dimension $3-\alpha$. This conclusion agrees well with the data reported in [10], where the more powerful streamwise vortices are indeed not space filling. One could even hypothesize that, as the streamwise vortices meander, the transverse vortices that produce u can be identified at least in part with transverse components of vortices that are mostly streamwise.

An interpretation of these observations is suggested by the discussion in [37]. The process that occurs in a wall layer is a transfer of momentum or impulse from the outer regions to the wall, or, equivalently, a transfer of impulse of opposite polarity from the wall to the interior. This transfer is intermittent, concentrated in localized bursts which create a vorticity scale different from y, consistent with the power law (4.9).

Note that as Re tends to infinity, α tends to zero. One should be very careful not to conclude from this that as the viscosity tends to zero the power law somehow converges to the von Kármán-Prandtl universal logarithmic law. As was already pointed out above, as the viscosity tends to zero the scaling law converges to the *upper* branch of the chevron. This upper branch then covers most of the pipe's cross-section, and in the limit of vanishing viscosity corresponds to a highly intermittent vorticity field concentrated on very thin, very strong and very folded vortices. No length scale can be assigned to this limiting vorticity field other than an external scale which in the present case is y. As the viscosity becomes finite the various processes associated with it, *eg* smoothing, cancellation of hairpin vortices and reconnection, create coherent vortices with a distinct vortical length scale associated with the exponent α. One can view our scaling law as a small-viscosity perturbation of the very intermittent flow that generates the upper branch of the chevron.

A scaling analysis similar to the one offered above can also be carried out for the inertial range of local structure in turbulence, where it leads to the Kolmogorov-Obukhov scaling laws as well as to a novel analysis of the effects of intermittency. This analysis is presented elsewhere. More generally, we wish to point out that our use of advanced similarity methods together with an asymptotic expansion based on a statistical argument constitutes a step towards an analysis of turbulence from first principles.

ACKNOWLEDGMENT

We would like to thank the following persons for helpful discussions, suggestions, or help with the data: DG Friend, N Goldenfeld, OH Hald, M Hites, F Hussain, H Nagib, and C Ward.

REFERENCES

1. Barenblatt GI (1979), *Similarity, Self-Similarity and Intermediate Asymptotics*, Consultants Bureau, NY.
2. Barenblatt GI (1991), Scaling laws (incomplete self-similarity with respect to Reynolds numbers) for the developed turbulent flows in pipes, *CR Acad Sc Paris*, series II, **313**, 307-312.
3. Barenblatt GI (1993), Scaling laws for fully developed turbulent shear flows. Part 1: Basic hypotheses and analysis, *J Fluid Mech* **248**, 513-520.
4. Barenblatt GI and Chorin AJ (1996), Small viscosity asymptotics for the inertial range of local structure and for the wall region of wall-bounded turbulence, *Proc Nat Acad Sci* **93**, 6749-6752.
5. Barenblatt GI and Chorin AJ (1997), Scaling laws and vanishing viscosity limits for wall-bounded shear flows and for local structure in developed turbulence, *Comm Pure Appl Math* **50**, 381-398.
6. Barenblatt GI and Chorin AJ (1996), Scaling laws and vanishing viscosity limits in turbulence theory, *Proc Venice Conf in honor of P Lax and L Nirenberg*, (in press).
7. Barenblatt GI, Chorin AJ, and Prostokishin VM (1997), Scaling laws in turbulent pipe flow: Discussion of experimental data, *Proc Natl Acad Sci* **94**, 773-776.
8. Barenblatt GI and Goldenfeld N (1995), Does fully developed turbulence exist? Reynolds number dependence vs asymptotic covariance, *Phys Fluids A*, 3078-3082.
9. Barenblatt GI and Prostokishin VM (1993), Scaling laws for fully developed shear flows - Part 2: Processing of experimental data, *J Fluid Mech* **248**, 521-529.
10. Bernard P, Thomas J, and Handler R (1993), Vortex dynamics and the production of Reynolds stress, *J Fluid Mech* **253**, 385-419.
11. Bradshaw P and Huang GP (1995), Law of the wall in turbulent flow, *Proc Royal Soc London A* **451**, 165-188.
12. Brown G (1991), ARPA-URI proposal, Princeton Univ.
13. Chorin AJ (1991) Equilibrium statistics of a vortex filament with applications, *Comm Math Phys* **141**, 619-631.
14. Chorin AJ (1994), *Vorticity and Turbulence*, Springer.
15. Chorin AJ (1996), Turbulence as a near-equilibrium process, *Lectures in Appl Math* **31**, 235-248.
16. Chorin AJ (1996), Turbulence cascades across equilibrium spectra, *Phys Rev E* **54**, 2616-2619.
17. Chorin AJ (1996), Onsager's contribution to turbulence theory: Vortex dynamics and turbulence in ideal flow, in L Onsager, Collected Works with Commentary, Hemmer P *et al* (eds), World Scientific.
18. Coles D (1956), Law of the wall in the turbulent boundary layer, *J Fluid Mech* **1**, 191-226.
19. Fernholz HH and Finley PJ (1996), Incompressible zero-pressure-gradient turbulent boundary layer: An assessment of the data, *Prog Aerospace Sci* **32**, 245-311.
20. Friend DG (1996), Calculations using the AIRPROPS program, NIST, Boulder, CO.
21. Gad-el-Hak M and Bandyopadhyay PR (1994), Reynolds number effects in wall-bounded turbulent flows, *Appl Mech Rev* **47**, 307-366.
22. Goldenfeld N (1992), *Lectures on Phase Transitions and the Renormalization Group*, Addison-Wesley, Reading, MA.
23. Hites M (1997), Scaling of the high-Reynolds number turbulent boundary layer, PhD Thesis, Illinois Institute of Technology.
24. Hussain F, Kambe T, Kuwahara K, and Orszag S (1991), Challenges in turbulence research, *Fluid Dyn Res* **7**, 51-63.
25. von Kármán T (1932), Mechanische Aehnlichkeit und Turbulenz, *Nach Ges Wiss Goettingen Math-Phys Klasse*, 58-76.

26. Kailasnath P (1993), Reynolds number effects and the momentum flux in turbulent boundary layers, PhD thesis, Yale University.
27. Kline SJ, Reynolds WC, Schraub FA, and Rundstadler PW (1967), Structure of turbulent boundary layers, J *Fluid Mech* **30**, 741-774.
28. Landau LD and Lifshitz EM (1959), *Fluid Mechanics*, Pergamon, NY.
29. Monin AS and Yaglom AM (1971), *Statistical Fluid Mechanics*, Vol 1, MIT Press, Boston, MA.
30. Nagib H and Hites M (1995), High Reynolds number boundary layer measurements in the NDF, AIAA paper 95-0786, Reno, NV.
31. Nikuradze J (1932), Gesetzmaessigkeiten der turbulenten Stroemung in glatten Rohren, *VDI Forschunghefl*, No 356.
32. Onsager L (1950), Distribution of energy in turbulence, *Phys Rev* **68**, 286.
33. Prandtl L (1932), Zur turbulenten Stroemung in Rohren und laengs Platten, *Ergeb Aerodyn Versuch*, Series 4, Goettingen.
34. Rott N (1990) Note on the history of the Reynolds number, *Ann Rev Fluid Mech* **22**, 1-11.
35. Schlichting H (1968), *Boundary Layer Theory*, McGraw-Hill, NY, Second Edition.
36. Sreenivasan KR (1987), Unified view of the origin and morphology of turbulent boundary layer structure, *IUTAM Symp*, Bangalore, Liepmann HW and Narasimha R (eds).
37. Sreenivasan KR (1989), Turbulent boundary layer, *Frontiers in Experimental Fluid Mechanics*, Gad-el-Hak M (ed), Springer, 159-209.
38. Zagarola MV, Smits AJ, Orszag SA, and Yakhot V (1996), Experiments in high Reynolds number turbulent pipe flow, AIAA paper 96-0654, Reno, NV.
39. Zagarola MV (1996), Mean flow scaling in turbulent pipe flow, PhD Thesis, Princeton Univ.

Grigory Isaakovich Barenblatt *graduated from the Department of Mechanics and Mathematics, Moscow University, where he received his MS, PhD, and DSc degrees. He has worked in the Soviet Academy of Sciences (at the Institute of Petroleum and Institute of Oceanology), Moscow University, and Moscow Institute of Science and Technology. He was the first recipient of the GI Taylor Chair of Fluid Mechanics at the University of Cambridge (since 1995 Professor Emeritus). Barenblatt has been Professor of Mathematics at the University of California, Berkeley since 1997. He is a Foreign Member of the American Academy of Arts and Sciences, Foreign Associate of the US National Academy of Engineering, Foreign Associate of the US National Academy of Sciences, Member of the European Academy, and Laureate of Modesto Panetti Medal and Prize.*

Alexandre J Chorin *received his engineering Diploma from the Institute of Technology in Lausanne, Switzerland, and his PhD in mathematics from the Courant Institute in New York. He is Professor of Mathematics at the University of California, Berkeley, and Senior Research Scientist at the Lawrence Berkeley National Laboratory. He is a Member of the National Academy of Sciences, a Fellow of the American Academy of Arts and Sciences, and a recipient of the National Academy's Award in applied mathematics and numerical analysis.*

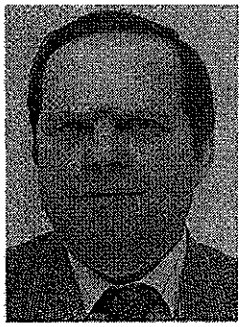

Valery Mikhailovich Prostokishin *received his MS Diploma from the Department of Mathematics and Physics, Latvian State University, Riga, and his PhD in physics and mathematics from the Moscow Engineering Physics Institute. He continued his work at Moscow Engineering Physics Institute as Associate Professor. Since 1990, he has been Senior Research Scientist at the PP Shirshov Institute of Oceanology, Russian Academy of Sciences.*